



**Quasi-Euclidean Recovery from Unknown but Complete Orbital  
Motion**

*Sing Bing Kang*

Cambridge  
Research  
Laboratory

**Cambridge Research Laboratory**

Technical Report Series

**CRL 97/10**

October 1997

---

## Cambridge Research Laboratory

The Cambridge Research Laboratory was founded in 1987 to advance the state of the art in both core computing and human-computer interaction, and to use the knowledge so gained to support the Company's corporate objectives. We believe this is best accomplished through interconnected pursuits in technology creation, advanced systems engineering, and business development. We are actively investigating scalable computing; mobile computing; vision-based human and scene sensing; speech interaction; computer-animated synthetic persona; intelligent information appliances; and the capture, coding, storage, indexing, retrieval, decoding, and rendering of multimedia data. We recognize and embrace a technology creation model which is characterized by three major phases:

**Freedom:** The life blood of the Laboratory comes from the observations and imaginations of our research staff. It is here that challenging research problems are uncovered (through discussions with customers, through interactions with others in the Corporation, through other professional interactions, through reading, and the like) or that new ideas are born. For any such problem or idea, this phase culminates in the nucleation of a project team around a well articulated central research question and the outlining of a research plan.

**Focus:** Once a team is formed, we aggressively pursue the creation of new technology based on the plan. This may involve direct collaboration with other technical professionals inside and outside the Corporation. This phase culminates in the demonstrable creation of new technology which may take any of a number of forms - a journal article, a technical talk, a working prototype, a patent application, or some combination of these. The research team is typically augmented with other resident professionals—engineering and business development—who work as integral members of the core team to prepare preliminary plans for how best to leverage this new knowledge, either through internal transfer of technology or through other means.

**Follow-through:** We actively pursue taking the best technologies to the marketplace. For those opportunities which are not immediately transferred internally and where the team has identified a significant opportunity, the business development and engineering staff will lead early-stage commercial development, often in conjunction with members of the research staff. While the value to the Corporation of taking these new ideas to the market is clear, it also has a significant positive impact on our future research work by providing the means to understand intimately the problems and opportunities in the market and to more fully exercise our ideas and concepts in real-world settings.

Throughout this process, communicating our understanding is a critical part of what we do, and participating in the larger technical community—through the publication of refereed journal articles and the presentation of our ideas at conferences—is essential. Our technical report series supports and facilitates broad and early dissemination of our work. We welcome your feedback on its effectiveness.

Robert A. Iannucci, Ph.D.  
Director

# Quasi-Euclidean Recovery from Unknown but Complete Orbital Motion

Sing Bing Kang

October 1997

## Abstract

In this technical report, we address the problem of quasi-Euclidean reconstruction (i.e., close to scaled Euclidean but not necessarily exact) using an uncalibrated camera with a specific known type of motion, namely *unknown but complete orbital motion*. By orbital motion, we mean pure rotation about a fixed arbitrary axis. Exact scaled Euclidean reconstruction for orbital motion is not possible because of the 2 degree-of-freedom ambiguity [22]. We bypass the usual intermediate stages of projective or affine reconstruction and recover 3-D structure directly from point correspondences obtained from a two-stage bidirectional tracking process. 3-D reconstruction is done by applying the iterative Levenberg-Marquardt algorithm to minimize error between actual point tracks and projected point tracks. We show that reconstruction from complete orbital motion is superior to that from partial orbital motion. This work also investigates the sensitivity of recovered quasi-Euclidean reconstruction, tilt, and object rotation to the actual camera tilt.

**©Digital Equipment Corporation, 1997**

This work may not be copied or reproduced in whole or in part for any commercial purpose. Permission to copy in whole or in part without payment of fee is granted for nonprofit educational and research purposes provided that all such whole or partial copies include the following: a notice that such copying is by permission of the Cambridge Research Laboratory of Digital Equipment Corporation in Cambridge, Massachusetts; an acknowledgment of the authors and individual contributors to the work; and all applicable portions of the copyright notice. Copying, reproducing, or republishing for any other purpose shall require a license with payment of fee to the Cambridge Research Laboratory. All rights reserved.

CRL Technical reports are available on the CRL's web page at  
<http://www.crl.research.digital.com>.

Digital Equipment Corporation  
Cambridge Research Laboratory  
One Kendall Square, Building 700  
Cambridge, Massachusetts 02139

## Contents

<b>1</b>	<b>Introduction</b>	<b>1</b>
1.1	Prior work . . . . .	1
1.2	Quasi-Euclidean reconstruction from unknown but complete orbital motion . . . . .	3
1.3	Organization . . . . .	4
<b>2</b>	<b>General structure from motion</b>	<b>4</b>
2.1	Least-squares minimization . . . . .	5
2.2	Two-stage approach . . . . .	6
2.3	Initialization . . . . .	6
<b>3</b>	<b>Tracking</b>	<b>7</b>
<b>4</b>	<b>Sensitivity of reconstruction to tilt</b>	<b>8</b>
<b>5</b>	<b>Results</b>	<b>9</b>
5.1	Sequence of rotating synthetic cylindrical object . . . . .	9
5.2	Sequences of rotating real objects . . . . .	9
5.3	Complete rotation vs. incomplete rotation . . . . .	11
<b>6</b>	<b>Discussion</b>	<b>12</b>
<b>7</b>	<b>Summary</b>	<b>16</b>

## List of Figures

1	Graphs illustrating sensitivity of recovered (a) shape, (b) tilt angle, (c) local rotation angle, and (d) focal length, to the actual camera tilt during complete orbital motion. See text for a description of the conditions to which the experiments were subject. . . . .	10
2	Rotating synthetic cylinder (complete rotation, 40 frames): (a) 1st frame, (b) 5th frame, (c) top view, and (d) side view of recovered 3-D points (2291 points). . . . .	11
3	Rotating film box (complete rotation, 31 frames): (a) 1st frame, (b) 5th frame, (c) point tracks, (d)-(e) top, and side views of recovered 3-D points (1414 points). . . . .	12
4	Rotating film box (complete rotation, 31 frames): (a) 1st frame, (b) 5th frame, (c) point tracks, (d)-(f) top, front, and side views of recovered 3-D points (1414 points). . . . .	13
5	Rotating toy frog (complete rotation, 43 frames): (a) 1st frame, (b) 5th frame, (c) 2260 point tracks, (d)-(f) top, front, and side views of recovered 3-D points, (g)-(i) corresponding views of the actual toy frog. . . . .	14
6	Rotating cube (complete rotation, 48 frames): (a) first frame, (b) top view of recovered 3-D points (2500 points), (c) side view of 3-D points. . . . .	15
7	Rotating cube (not complete rotation): (a) First frame of the sequence, and (b) Top view of recovered points for the cube scene using 96 frames and known camera parameters. (From [25].) Notice the pinching effect. . . . .	15
8	Rotating synthetic cube: (a) Reconstruction from complete rotation, (b) Reconstruction from incomplete rotation. . . . .	16

# 1 Introduction

In this technical report, we address the problem of quasi-Euclidean reconstruction using an uncalibrated camera with the specific known type of motion, namely *unknown but complete orbital motion*. By orbital motion, we mean pure rotation about a fixed arbitrary axis. Exact scaled Euclidean reconstruction for orbital motion is not possible because of the 2 degree-of-freedom ambiguity [22]. We bypass the usual intermediate stages of projective or affine reconstruction and recover direct 3-D structure from point correspondences. The feature point correspondences are obtained from a two-stage bidirectional tracking process. 3-D reconstruction is done by applying the iterative Levenberg-Marquardt algorithm to minimize error between actual point tracks and projected point tracks. Initialization is based on estimating the tilt by fitting ellipses on point tracks and assuming equal angular rotation between frames. Convergence is speeded up by adopting an object-centered representation. This work is an extension of [25] with the projection function having the option of using all five camera intrinsic parameters (focal length  $f$ , aspect ratio  $r$ , image skew  $\sigma$ , and principal point  $(u_0, v_0)$ ). We also demonstrate that results from complete orbital motion are superior to those of partial orbital motion. This work also investigates the sensitivity of quasi-Euclidean reconstruction to the actual camera tilt during orbital motion.

## 1.1 Prior work

There is a large body of work done on 3-D reconstruction from images using an uncalibrated camera. One of the first steps taken prior to actual 3-D reconstruction is usually the process of camera calibration. Particularly germane to 3-D reconstruction using an uncalibrated camera is *self-calibration*. Self-calibration refers to recovery of camera parameters based only on correspondences of images taken at different poses. Most work done on self-calibration relies on known motions of the cameras, such as pure translational motion [2], known camera rotation angles [3], rotation about an unknown but fixed arbitrary axis [25], and pure rotation about the camera center [7].

The traditional approach to 3-D reconstruction with multiple images using an uncalibrated camera is to apply affine and projective reconstruction techniques (such as [4, 20, 6, 8]). The traditional approach to reconstruct scaled Euclidean structure is usually from known camera parameters. For example, Szeliski [23] and Matsumoto *et al.* [14] recover Euclidean structure from object rotation (or equivalently, camera orbital motion) using the assumption that the camera parameters and object motion are known. Niem and Wingbermühle [16] use a grided annulus pattern inside which the object is placed. Camera parameters are extracted from the detected pattern, and

the object is recovered from silhouettes. Zhang [26] proposes a closed-form solution for scaled Euclidean reconstruction with known intrinsic camera parameters but unknown extrinsic camera parameters. However, this technique assumes the existence of four coplanar correspondences that are not collinear.

Recently, however, there has been interesting work done in reconstructing scaled Euclidean structure from images using an uncalibrated camera. In a work that is probably the closest to ours, Heyden and Astrom [9] propose a technique to reconstruct scaled Euclidean structure under constant but unknown intrinsic camera parameters. They showed that in general, it takes a minimum of 3 images to recover a unique solution to the intrinsic camera parameters and scaled Euclidean structure. This is done by considering the *Kruppa constraints* [13, 15]. Their technique of scaled Euclidean reconstruction is based on recovering an intermediate projective structure. They then use an optimization formulation that is based on the Frobenius norm of a matrix. However, this is not equivalent to the more optimal metric of minimizing feature location errors in the 2-D image space. In a later work, they also show that scaled Euclidean reconstruction under known image aspect ratio and skew but varying and unknown focal length and principal point is also possible [10]. The assumption is that the camera is undergoing general motion, as it is not possible to reconstruct scaled Euclidean structure under constrained motion such as pure translational or orbital motion.

A two-step approach is used to recover scaled Euclidean structure from multiple image sequences with unknown but constant intrinsic parameters [18]. The first stage involves affine camera parameter recovery using the so-called *modulus* constraint. This is followed by conversion to scaled Euclidean structure. This approach is subsequently extended to remove the assumption of fixed camera focal length [17].

Hartley devises an algorithm for camera self-calibration from several views [5]. He uses a two-step approach to recover scaled Euclidean structure. His algorithm first recovers projective structure before applying a heuristic to search for extract the five intrinsic camera parameters. The heuristic involves iterating over several sets of initialization values and checking for convergence.

A detailed characterization of *critical motion sequences* (CMS) is given by Sturm [22]. A critical motion sequence is a camera motion sequence that results in ambiguities in reconstruction when camera parameters are unknown. For example, only affine structures can be extracted from pure camera translational motion. Of particular relevance to our work is the Sturm's determination that there is a two degree of freedom projective ambiguity for orbital motions (i.e., pure rotation about a fixed arbitrary axis).

## 1.2 Quasi-Euclidean reconstruction from unknown but complete orbital motion

As Sturm as demonstrated [22], there exists a 2 degree-of-freedom ambiguity in scaled Euclidean reconstruction. There are three options in recovering scaled Euclidean structure from orbital motion: (1) fix two intrinsic camera parameters, (2) impose structural constraints (e.g., orthogonality, parallelism, known 3-D locations of fiducial points), or (3) get the “best” reconstruction without (1) or (2). We choose to option (3), though option (1) is another convenient option as well. In particular, for option (1), we can assume that the aspect ratio  $r$  to be 1.0 and the image skew  $\sigma$  to be 0. In practice, these parameters are usually fixed for a camera and need to be determined only once.

We recover 3-D structure and orbital motion from relatively sparse sequence of images (typically between 30-50 images in a sequence). The unknowns are the camera intrinsic parameters, global camera tilt, local rotation axis, amount of local rotation between successive frames, and the 3-D positions associated with the tracked point features.

The assumptions that we have made for our work are the following:

- The image sequence is a “closed loop” sequence (i.e., featuring complete object rotation),
- The object surface has sufficient texture for interframe feature tracking,
- The object rotation is about an unknown but fixed axis, and
- The camera either does not have significant radial distortion, or the radial distortion factor is known so that the images can be corrected first.

The advantages of using our approach of recovering structure and motion from complete object rotation (or equivalently, complete camera orbital motion):

- The set-up is extremely simple and cheap (using a camera, tripod stand, and a turntable would do),
- The global tilt angle, local rotation angles, and quasi-Euclidean structure can be extracted simultaneously,
- Calibration of camera is not required,
- Initialization of the system is simple due to the known type of motion,

- Recovery of the intermediate affine or projective structure is not necessary, and
- The method exhibits fast convergence and is stable.

### 1.3 Organization

In Section 2, we outline the general structure from motion problem and our approach to recovering the solution specifically in the special case of unknown but complete orbital motion. The bidirectional tracking scheme employed to recover the point tracks for a given image sequences is described in Section 3. One of the important parameter in orbital motion is the amount of camera tilt. Section 4 shows, through simulations, how sensitive recovered shape and camera parameters are to the actual camera tilt. The results of reconstruction using image sequences of rotated simulated and real objects are given in Section 5. This section also illustrates the improvement in results due to the knowledge of complete camera orbital motion (or object rotation). The method and its results are discussed in Sections 6; finally, a summary of the method and its implications are presented in Section 7 respectively.

## 2 General structure from motion

The formulation of recovering structure from motion is based on that of [25]. Essentially, we are trying to recover a set of 3-D structure parameters  $\mathbf{p}_i$  and time-varying motion parameters  $T_j$  from a set of observed image features  $\mathbf{u}_{ij}$ . The general equation linking a 2D image feature location  $\mathbf{u}_{ij}$  in frame  $j$  to its 3-D position  $\mathbf{p}_i$  ( $i$  is the track index) is

$$\mathbf{u}_{ij} = \mathcal{P} \left( T_j^{(K)} \dots T_j^{(1)} \mathbf{p}_i \right) \quad (1)$$

where the perspective projection transformation  $\mathcal{P}()$  is applied to a cascaded series of rigid transformation  $T_j^{(k)}$ . Each transformation is in turn defined by

$$T_j^{(k)} \mathbf{x} = \mathbf{R}_j^{(k)} \mathbf{x} + \mathbf{t}_j^{(k)} \quad (2)$$

where  $\mathbf{R}^{(k)}$  is a rotation matrix and  $\mathbf{t}_j^{(k)}$  is a translation applied after the rotation.

Within each of the cascaded transforms, the motion parameters may be time-varying (the  $j$  subscript is present) or fixed (the subscript is dropped). The transformation associated with the (horizontal) orbital motion that we are considering in our work is

$$\mathbf{u}_{ij} = \mathcal{P} \left( \mathbf{R}_{x,\tau} \mathbf{R}_{z,\theta} \mathbf{p}_i + \mathbf{t} \right) \quad (3)$$

where  $\mathbf{R}_{x,\tau}$ ,  $\mathbf{R}_{z,\theta}$  represent rotation about the x-axis by  $\tau$  and z-axis by  $\theta$  respectively. We assume negligible cyclotorsion (rotation of camera about the viewing axis).

The general camera-centered perspective projection equation is

$$\begin{pmatrix} u \\ v \\ z \end{pmatrix} = \mathcal{P}_1 \begin{pmatrix} x \\ y \\ z \end{pmatrix} \equiv \begin{pmatrix} \frac{fx+\sigma y}{z} + u_0 \\ \frac{rfy}{z} + v_0 \\ z \end{pmatrix} \quad (4)$$

where  $f$  is a product of the focal length of the camera and the pixel array scale factor,  $r$  is the image aspect ratio,  $\sigma$  is the image skew, and  $(u_0, v_0)$  is the principal point.

An alternative object-centered formulation (a more general version of [25]) which we use is

$$\begin{pmatrix} u \\ v \\ z \end{pmatrix} = \mathcal{P}_2 \begin{pmatrix} x \\ y \\ z \end{pmatrix} \equiv \begin{pmatrix} \frac{sx+\eta\sigma y}{1+\eta z} + u_0 \\ \frac{rsy}{1+\eta z} + v_0 \\ z \end{pmatrix} \quad (5)$$

Here, we assume that the  $(x, y, z)$  coordinates before projection are with respect to a reference frame that has been displaced away from the camera by a distance  $t_z$  along the optical axis,<sup>1</sup> with  $s = f/t_z$  and  $\eta = 1/t_z$ . The projection parameter  $s$  can be interpreted as a *scale factor* and  $\eta$  as a *perspective distortion factor*. Our alternative perspective formulation results in a more robust recovery of camera parameters under weak perspective, where  $\eta \ll 1$ , and assuming  $(u_0, v_0) \approx (0, 0)$  and  $\sigma \approx 0$ , we have  $\mathcal{P}(x, y, z)^T \approx (sx, rsy)^T$ . This is because  $s$  and  $rs$  can be much more reliably recovered than  $\eta$ , in comparison with the old formulation where  $f$  and  $t_z$  are very highly correlated.

## 2.1 Least-squares minimization

The Levenberg-Marquardt algorithm [19] is used to solve for the structure and motion parameters. The merit or objective function that we minimize is

$$\mathcal{C}(\mathbf{a}) = \sum_i \sum_j c_{ij} |\mathbf{u}_{ij} - \mathbf{f}(\mathbf{a}_{ij})|^2, \quad (6)$$

where  $\mathbf{f}()$  is given in (1) and

$$\mathbf{a}_{ij} = (\mathbf{p}_i^T, \mathbf{m}_j^T, \mathbf{m}_g^T)^T \quad (7)$$

---

<sup>1</sup>If we wish, we can view  $t_z$  as the  $z$  component of the original global translation which is absorbed into the projection equation, and then set the third component of  $\mathbf{t}$  to zero.

is the vector of structure and motion parameters which determine the image of point  $i$  in frame  $j$ . The vector  $\mathbf{a}$  contains all of the unknown structure and motion parameters, including the 3-D points  $\mathbf{p}_i$ , the time-dependent motion parameters  $\mathbf{m}_j$ , and the global motion/calibration parameters  $\mathbf{m}_g$ . The weight  $c_{ij}$  in (6) describes our confidence in measurement  $\mathbf{u}_{ij}$ , and is normally set to the inverse variance  $\sigma_{ij}^{-2}$ . Implementational details are given in [25]. The primary difference between their work and this work is that we incorporate the additional camera intrinsic parameters  $r$ ,  $\sigma$ ,  $u_0$ , and  $v_0$ . The extensions (calculating the required derivatives of the Hessian matrix and gradient vector) are relatively straightforward.

## 2.2 Two-stage approach

As Sturm has shown [22], there is a 2 degree-of-freedom ambiguity in scaled Euclidean reconstruction for orbital motion. A simple solution to this is to set two of the intrinsic camera parameters to a constant (either as an assumption or through calibration). A good choice would be to fix the image skew factor  $\sigma$  (say to 0) and the aspect ratio  $r$  (say to 1). However, in our work, we keep these parameters unknown.

We use a two-step approach in acquiring the quasi-Euclidean structure:

- Fix  $\sigma = u_0 = v_0 = 0$  and  $r = 1$  and apply the Levenberg-Marquardt algorithm until terminating conditions are met. The termination conditions are either the number of iterations exceeds a threshold (150 in our case) or the improvement in the objective function is too small ( $10^{-6}$  in our case), whichever comes first.
- Set  $\sigma$ ,  $u_0$ ,  $v_0$ , and  $r$  to be free variables and resume with Levenberg-Marquardt algorithm (with the iteration number reset to 0) until the same termination conditions are again met.

In general, using this two-step approach has resulted in better convergence towards lower image projection errors and better structure and motion recovery in comparison to not applying the first step. This observation is based on more than 100 runs that involve synthetic image sequences and about 6 runs involving real image sequences.

## 2.3 Initialization

The initialization of object motion for each frame is made simpler by the fact that we know that object motion is a rotation about a unique (but unknown) axis. If there are  $N_{\text{frame}}$  images in the sequence, then the local rotation angle about the z-axis associated with image  $j$  is initialized to

$\frac{360^\circ i}{N_{\text{frame}}}$ . The camera tilt is estimated by fitting ellipses to the tracks. The estimated tilt used for initialization is usually within  $15^\circ$  of the actual camera tilt (based on simulation results).

The scale factor  $s$  and perspective distortion factor  $\eta$  are initialized to arbitrary values of 1.0 and 0.001 respectively. The algorithm does not appear to be too sensitive to these values, as changes up to about an order of magnitude is tolerated.

### 3 Tracking

To produce tracks in a circular sequence as input to the iterative least-squares minimizing procedure, we first mask out regions that do not change significantly in intensity through simple pairwise image subtraction. This is effective in removing the static background and low object texture areas.

The tracking then proceeds by way of bidirectional tracking with three stages:

1. Pairwise global spline-based registration [24],
2. Automatic selection of spline node points with high local texture,
3. Multiframe Shi-Tomasi local tracking [21] of these spline nodes.

These three stages are necessary to incorporate the advantages of both spline-based registration and local tracking techniques. While the spline-based registration technique is able to track relatively significant motion, it is not able to deal with motion discontinuity very well due to its implicit smoothness constraint. On the other hand, the local tracking technique performs very poorly for significant motion but very well within the vicinity of the true track position. Because points are tracked independently for local tracking, motion discontinuities can be handled. Since the spline-based registration technique yields a reasonably good estimate of motion, the local tracking technique can then make use of this estimate to improve on the new track image position, especially if the position is within the vicinity of a motion discontinuity.

In the first stage, image flow between successive frames in the circular sequence is computed in both directions using the spline-based registration technique. Then, in stage 2, for each frame, points with high local texture (indicated by the minimum eigenvalue of the local Hessian) are automatically chosen for tracking. Finally, at the third and final stage of tracking, for every frame, the chosen points are then individually locally tracked *in both directions* using the flow estimates from stage 1. The tracking stops (tracking in the two directions is independent) if any of the following conditions is violated:

- Each trace continuously move in one direction,

- The RMS pixel difference error is less than a threshold (15 in our case), or
- The minimum eigenvalue is above a threshold (500 in our case).

The problem with the first criterion above is that a complete track that is observable in all the frames is not possible. However, the need to reject random noise is greater, and having a few more redundant points is a relatively small price to pay. The tracks are postprocessed to remove those that are deemed too short (we impose a minimum track length of 3).

## 4 Sensitivity of reconstruction to tilt

To ensure that the ground truth is available, experiments were conducted using a collection of synthetic 3-D points. The 3-D points were generated at random, and the only constraint on their location is that they have to be within a radius of 25 from its local center. The object local center is chosen to be a distance of 225 from the camera center. Each 3-D point is oriented, i.e., each point has a normal associated with it. This allows “visibility” to be determined based on the camera pose; a point  $\mathbf{p}_i$  with normal  $\hat{\mathbf{n}}_i$  is visible under camera pose  $j$  if  $\hat{\mathbf{n}}_i \cdot \hat{\mathbf{z}}_{j,\text{cam}} \leq 0$ .  $\hat{\mathbf{z}}_{j,\text{cam}}$  is the  $j$ th unit camera viewing direction away from the camera. Tracking is not explicitly done here, since we can calculate the 2-D image coordinates directly based on known camera and object transformations. Structure from orbital motion is then performed on the artificial tracks, with different image (Gaussian) noise levels.

The RMS error in recovered 3-D is calculated by finding

$$\mathcal{E} = \min \sum_{i=1}^{N_{\text{points}}} \|\mathbf{p}_{i,\text{cor}} - m\mathbf{R}\mathbf{p}_i - \mathbf{c}\|^2 \quad (8)$$

and taking the square root of  $\mathcal{E}$ .  $N_{\text{points}}$  is the number of points, and  $\mathbf{p}_{i,\text{cor}}$  and  $\mathbf{p}_i$  the theoretically correct and recovered  $i$ th point respectively.  $m$  is the global scale,  $\mathbf{R}$  the global rotation, and  $\mathbf{c}$  the global translation; these parameters constitute the best rigid body transformation between the theoretically correct and recovered set of points. We implemented Horn’s algorithm that uses a closed-form solution for this least-squares problem [11]. An alternative method that can be used is based on singular value decomposition (SVD) of a  $3 \times 3$  matrix [1].

We ran experiments involving a variety of gaussian image noise, namely, 0.0, 0.1, 0.3, 0.5, 1.0, and 2.0 pixels. As a reference, the projected 3-D points are distributed within an area of approximately  $60 \times 60$  pixels. The results of the experiment are graphically shown in Figure 1. For this figure, note that the local rotation is constrained to be about the z-axis. To reiterate, as a point

of reference for the graph shown in Figure 1(a), the 3-D points are randomly distributed within a ball of radius of 25, and the center of this ball is a distance of 225 away from the center of the camera. The actual focal length is 324.

As can be seen in Figure 1, the error in recovered shape and tilt generally increases with the camera tilt. There are two surprises: (1) the very gradual increase in error followed by a very sharp increase in error with increasing actual camera tilt, and (2) the error in the local rotation angle estimate does not seem to exhibit a consistent trend. The sharpness of the reciprocal trend in (1) is somewhat attenuated by noise, as shown in Figure 1(a).

## 5 Results

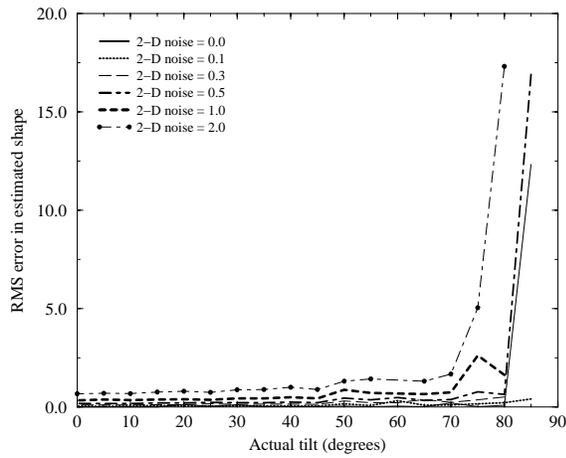
In this section, we present results using a synthetic object as well as several real objects. In addition, we compare results obtained from complete rotation with those from the exact same sequence, but without the completeness of rotation assumption. The initialization is the same for both cases.

### 5.1 Sequence of rotating synthetic cylindrical object

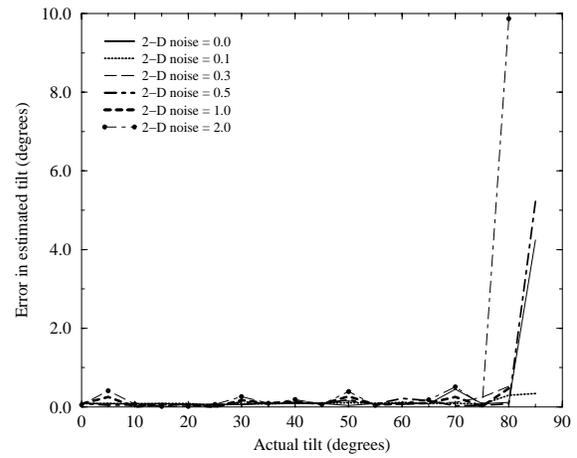
In the previous synthetic examples, the tracks were computed directly from known camera parameters. In this example, however, a textured cylinder was defined, rotated, and then rendered using Rayshade. (Rayshade is a program for producing ray-traced color images [12].) The sequence of images produced in this manner is then treated as a normal input sequence whose bidirectional point tracks are recovered and fed into the “structure from complete orbital motion” module. The camera tilt is maintained at  $0^\circ$ , and there are 40 frames in this sequence (two of which are shown in Figure 2(a) and (b)). Two views of the reconstructed 3-D points are shown in Figure 2(c) and (d). The average (best-fit) cross-sectional radius of the recovered points is 0.823869, while the RMS error of the fit in radius is 0.063680. Since the actual radius of cylinder is 1.0, the rescaled RMS error of radius fit is 0.077293842. Because the distance of the cylinder from the camera is 8.0, the rescaled RMS error of radius fit of the recovered set of 3-D points constitute only about 1% of the camera distance.

### 5.2 Sequences of rotating real objects

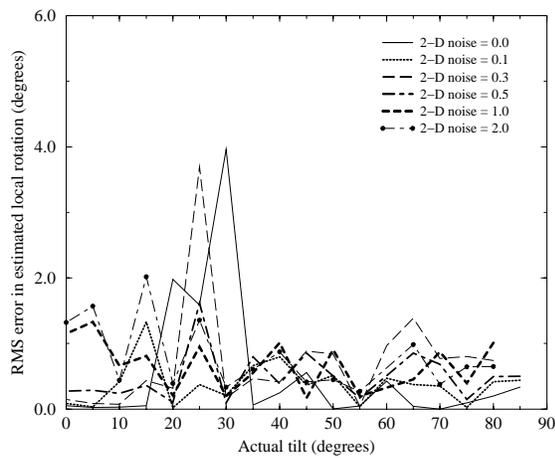
In this section, we show results of applying the technique to four image sequences of real objects, namely a dodecahedron (Figure 3), a film box (Figure 4), a toy frog (Figure 5), and a cube (Figure 6).



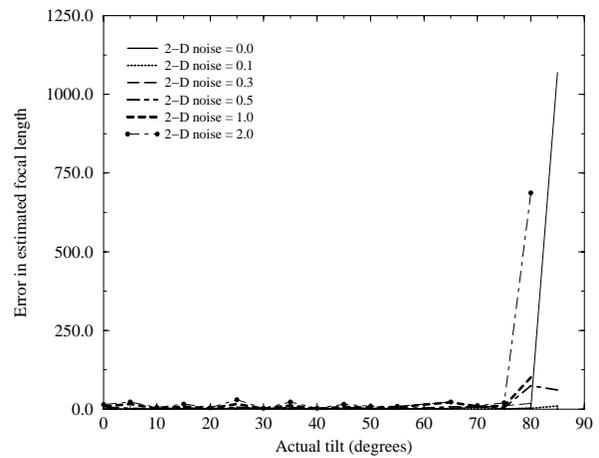
(a)



(b)



(c)



(d)

Figure 1: Graphs illustrating sensitivity of recovered (a) shape, (b) tilt angle, (c) local rotation angle, and (d) focal length, to the actual camera tilt during complete orbital motion. See text for a description of the conditions to which the experiments were subject.

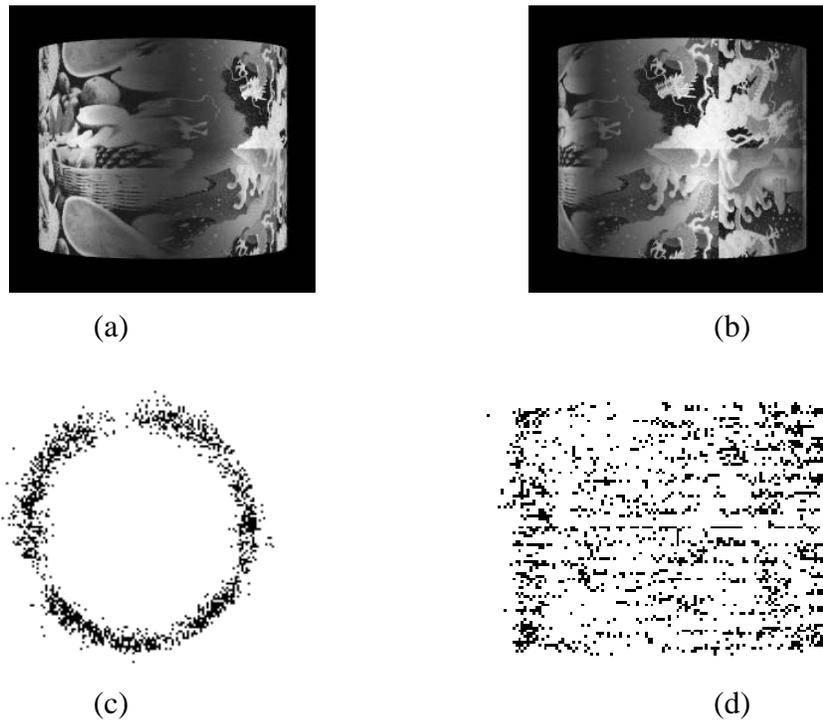


Figure 2: Rotating synthetic cylinder (complete rotation, 40 frames): (a) 1st frame, (b) 5th frame, (c) top view, and (d) side view of recovered 3-D points (2291 points).

As can be seen, the 3-D points for all these sequences have been recovered reasonably well. The film box was the most difficult sequence, since the surface of the box is highly specular. This resulted in noisier 3-D position estimates (Figure 4). In addition, it can be observed from Figures 3-5 that the point traces are not all correct. Outlier rejection was used in the Levenberg-Marquardt to remove points that may be wrongly tracked.

### 5.3 Complete rotation vs. incomplete rotation

Most work on structure from rotation do not use complete rotation. For the same number of frames, it is logical to deduce that with complete rotation, with a circular sequence where the first and last frames are adjacent, the reconstruction is better due to the extra constraints for feature points between these frames and their vicinities. As an illustration, Figure 7 shows the result of applying normal structure from incomplete rotation. The errors in estimating the rotation angles are all biased in one direction due to the single “open” chain of constraints, causing the “pinched” appearance. In comparison, the reconstructed 3-D points of the same object under complete rotation

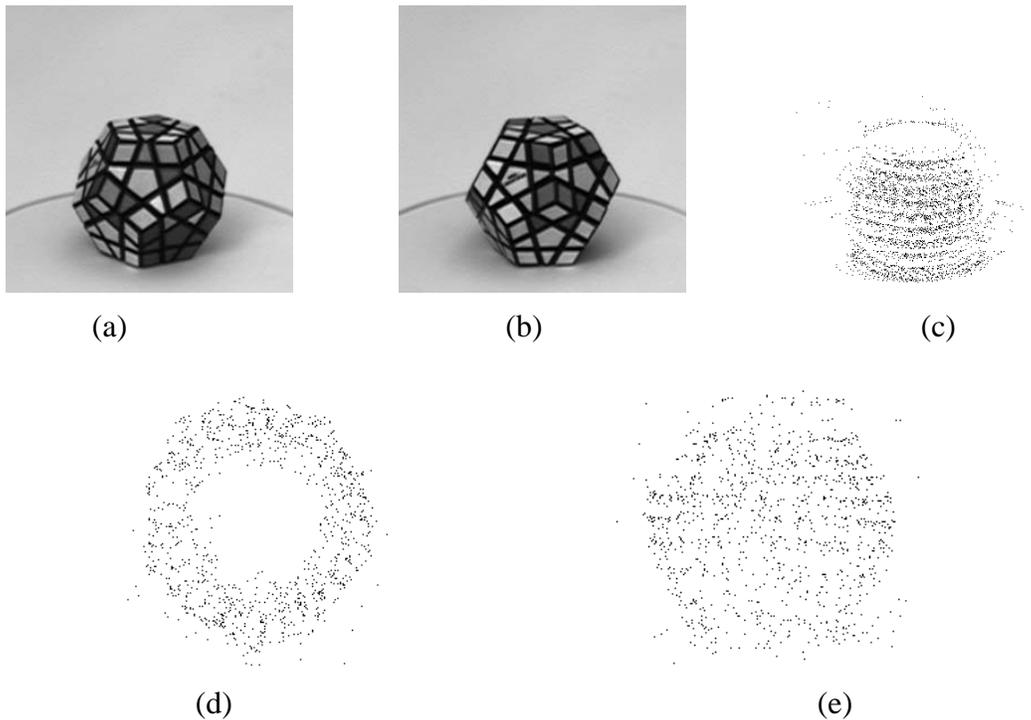


Figure 3: Rotating film box (complete rotation, 31 frames): (a) 1st frame, (b) 5th frame, (c) point tracks, (d)-(e) top, and side views of recovered 3-D points (1414 points).

(Figure 6) do not result in the same “pinched” appearance.

Another example is shown in Figure 8. Figure 8(a) shows the top view of the reconstructed 3-D points for the case when complete rotation is assumed, while Figure 8(b) shows the same points for the case when complete rotation is not assumed. In this case, each track that spans across the first and last frames is first broken up into two shorter tracks. The longer of the two fragmented tracks is used while the other is discarded. Not surprisingly, the reconstructed 3-D points for the complete rotation case is better. There are 416 points on the cube, and the camera tilt is  $45^\circ$  for both cases. The tracks were synthetically generated with no noise, and there were 45 frames with equiangularly spaced object rotation. Initialization for both cases is exactly the same.

## 6 Discussion

Despite reconstruction ambiguities that exist to orbital motion, we have shown, through synthetic and real scenes, that reasonable quasi-Euclidean reconstruction can be done. This is because in

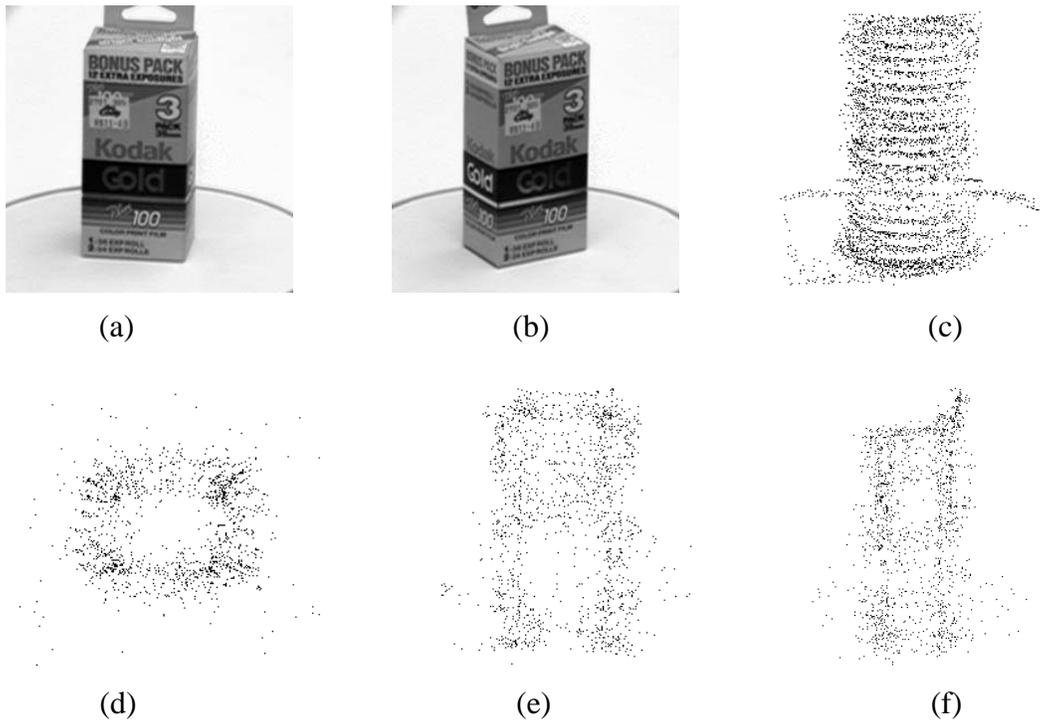


Figure 4: Rotating film box (complete rotation, 31 frames): (a) 1st frame, (b) 5th frame, (c) point tracks, (d)-(f) top, front, and side views of recovered 3-D points (1414 points).

practice, the camera intrinsic parameters of principal point  $(u_0, v_0)$ , image skew  $\sigma$ , and aspect ratio  $r$  do not usually deviate significantly from normally assumed values of  $(0, 0)$ ,  $0$ , and  $1$  respectively. We operate based on our preference of maximizing knowledge of the camera to directly reconstructing 3-D shape, rather than converting to intermediate projective or affine representations.

Results of experiments with simulated tracks having varying degrees of image feature location noise and actual camera tilt (relative to the vertical axis) were generally expected, with some surprises. While errors in estimated reconstructed shape, camera tilt, and focal length increased with actual camera tilt, the rate of increase in these errors is unexpected. The rate of increase in error is generally gradual up until angles close to  $90^\circ$ , when the rate suddenly shoots up. This suggests that any reasonable tilt angle is acceptable without significant degradation in the fidelity of 3-D reconstruction and motion recovery. Another surprise is the insensitivity of errors (based on their apparent randomness in the results) in estimated local rotation angles with both image noise and actual camera tilt.

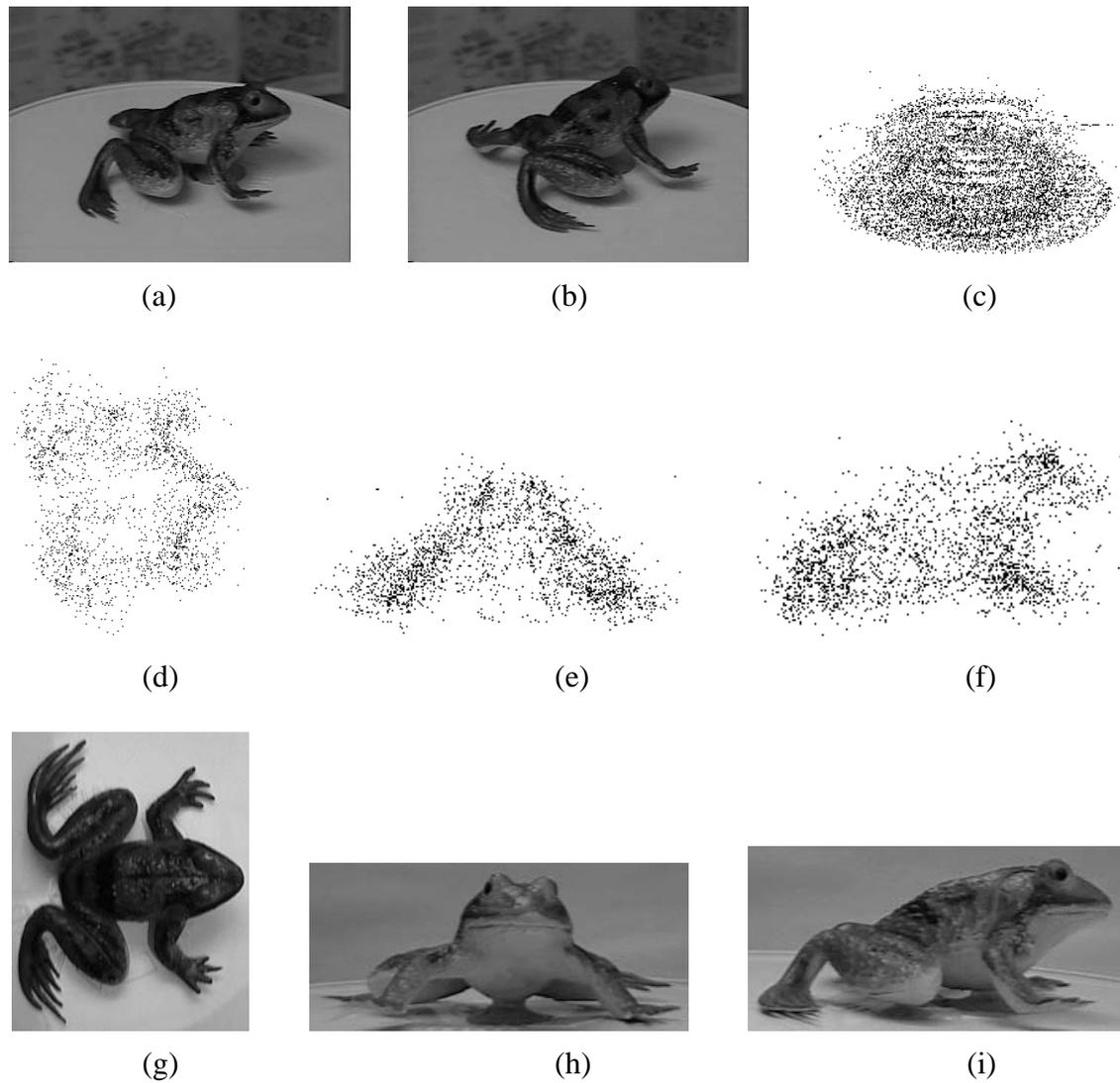


Figure 5: Rotating toy frog (complete rotation, 43 frames): (a) 1st frame, (b) 5th frame, (c) 2260 point tracks, (d)-(f) top, front, and side views of recovered 3-D points, (g)-(i) corresponding views of the actual toy frog.

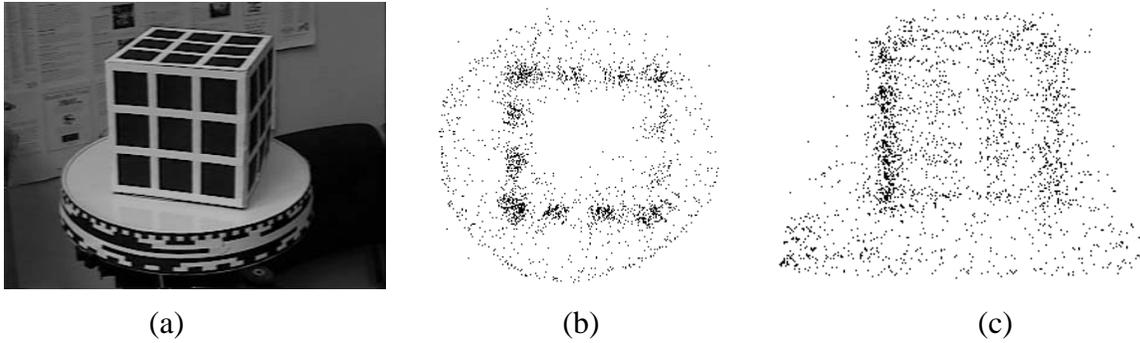


Figure 6: Rotating cube (complete rotation, 48 frames): (a) first frame, (b) top view of recovered 3-D points (2500 points), (c) side view of 3-D points.

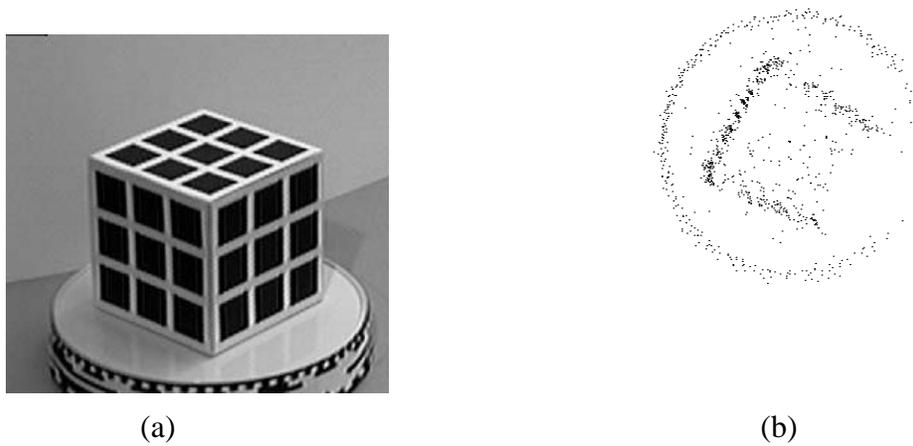


Figure 7: Rotating cube (not complete rotation): (a) First frame of the sequence, and (b) Top view of recovered points for the cube scene using 96 frames and known camera parameters. (From [25].) Notice the pinching effect.

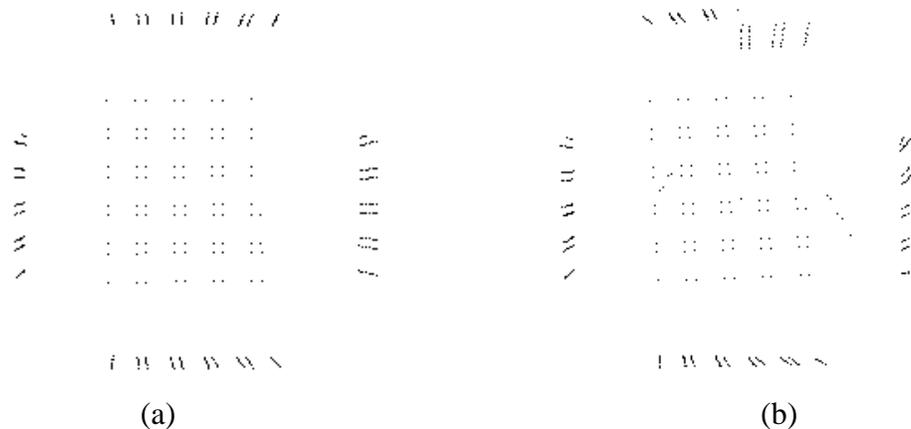


Figure 8: Rotating synthetic cube: (a) Reconstruction from complete rotation, (b) Reconstruction from incomplete rotation.

Finally, not surprisingly, results for experiments with the assumption that the object rotation (or equivalently, camera orbital motion) spans a full  $360^\circ$  are better than those with no such assumption. The better results are due to the additional constraints available in connection with the point tracks that bridge the first and last frames of the (circular) image sequence. One can anticipate that in the general case, structure and motion recovery from arbitrary but “closed loop” motion of the camera would be more accurate than if there is no assumption of direct connectedness between the first and last frames of the image sequence.

## 7 Summary

We have described a completely automatic method of recovering quasi-Euclidean structure from unknown by complete object rotation (or equivalently, camera orbital motion). This method starts with two-stage bidirectional tracking, followed by the application of iterative Levenberg-Marquardt minimization of feature point error to recover structure and rotational motion simultaneously. Apart from the knowledge that the object was rotated completely about a unique axis, no other camera parameters are assumed known.

This technique directly locally minimizes the error between the projected image feature position and measured feature position, and no intermediate affine or projective reconstruction is done. This technique usually converges toward the correct solution due to the assumption of complete object rotation, which makes simplifies initialization. In addition, because we know the motion is that of rotation, we can always make a good initial estimate of the camera tilt by fitting ellipses on

the recovered tracks.

Simulations have indicated the surprising result that the recovered errors in shape, tilt, and focal length exhibit a very sharp reciprocal relationship with respect to the actual camera tilt. The sharpness is attenuated by 2-D feature location (gaussian) noise. Another interesting result of the same simulations is the relative indifference of errors in recovered local rotation angles to both actual camera tilt and noise. Applying the technique on image sequences of real rotated objects has yielded very reasonable-looking results of recovered 3-D object feature distribution.

## References

- [1] K.S. Arun, T.S. Huang, and S.D. Blostein. Least-squares fitting of two 3-D point sets. *IEEE Transactions on Pattern Analysis and Machine Intelligence*, 9(5):698–700, September 1987.
- [2] L. Dron. Dynamic camera self-calibration from controlled motion sequences. In *IEEE Computer Society Conference on Computer Vision and Pattern Recognition (CVPR'93)*, pages 501–506, New York, NY, June 1993. IEEE Computer Society Press.
- [3] F. Du and M. Brady. Self-calibration of the intrinsic parameters of cameras for active vision systems. In *IEEE Computer Society Conference on Computer Vision and Pattern Recognition (CVPR'93)*, pages 477–482, New York, NY, June 1993. IEEE Computer Society Press.
- [4] O. D. Faugeras. What can be seen in three dimensions with an uncalibrated stereo rig? In *Second European Conference on Computer Vision (ECCV'92)*, pages 563–578, Santa Margherita Liguere, Italy, May 1992. Springer-Verlag.
- [5] R. I. Hartley. An algorithm for self calibration from several views. In *IEEE Computer Society Conference on Computer Vision and Pattern Recognition (CVPR'94)*, pages 908–912, Seattle, Washington, June 1994. IEEE Computer Society.
- [6] R. I. Hartley. Projective reconstruction and invariants from multiple images. *IEEE Transactions on Pattern Analysis and Machine Intelligence*, 16(10):1036–1041, October 1994.
- [7] R. I. Hartley. Self-calibration from multiple views with a rotating camera. In *Third European Conference on Computer Vision (ECCV'94)*, volume 1, pages 471–478, Stockholm, Sweden, May 1994. Springer-Verlag.

- [8] A. Heyden. Reconstruction from image sequences by means of relative depths. In *Fifth International Conference on Computer Vision (ICCV'95)*, pages 1058–1063, Cambridge, Massachusetts, June 1995. IEEE Computer Society Press.
- [9] A. Heyden and K. Astrom. Euclidean reconstruction from constant intrinsic parameters. In *Proc.s 13th International Conference on Pattern Recognition*, pages 339–343, 1996.
- [10] A. Heyden and K. Astrom. Euclidean reconstruction from image sequences with varying and unknown focal length and principal point. In *Proc.s IEEE Computer Society Conference on Computer Vision and Pattern Recognition*, pages 438–443, June 1997.
- [11] B. K. P. Horn. Closed-form solution of absolute orientation using unit quaternions. *Journal of the Optical Society of America A*, 4(4):629–642, 1987.
- [12] C. E. Kolb. *Rayshade User's Guide and Reference Manual*, August 1994.
- [13] E. Kruppa. Objektes aus zwei perspektiven mit innerer orientierung. *Sitz.-Ber. Akad. Wiss., Math. Naturw. Kl., Abt. Ila.*, 122:1939–1948, 1913.
- [14] Y. Matsumoto, H. Terasaki, K. Sugimoto, and T. Arakawa. A portable three-dimensional digitizer. In *International Conference on Recent Advances in 3-D Digital Imaging and Modeling*, pages 197–204, Ottawa, Canada, May 1997.
- [15] S. Maybank. *Theory of Reconstruction from Image Motion*. Springer-Verlag, Berlin, 1993.
- [16] W. Niem and J. Wingbermhle. Automatic reconstruction of 3D objects using a mobile monoscopic camera. In *International Conference on Recent Advances in 3-D Digital Imaging and Modeling*, pages 173–180, Ottawa, Canada, May 1997.
- [17] M. Pollefeys, L. Van Gool, and A. Oosterlinck. Euclidean reconstruction from image sequences with variable focal length. In *Fourth European Conference on Computer Vision (ECCV'96)*, volume 1, pages 31–44, Cambridge, England, April 1996. Springer-Verlag.
- [18] M. Pollefeys, L. Van Gool, and A. Oosterlinck. The modulus constraint: A new constraint for self-calibration. In *Proc.s 13th International Conference on Pattern Recognition*, volume 1, pages 349–353, 1996.
- [19] W. H. Press, B. P. Flannery, S. A. Teukolsky, and W. T. Vetterling. *Numerical Recipes in C: The Art of Scientific Computing*. Cambridge University Press, Cambridge, England, second edition, 1992.

- [20] A. Shashua. Projective structure from uncalibrated images: Structure from motion and recognition. *IEEE Transactions on Pattern Analysis and Machine Intelligence*, 16(8):778–790, August 1994.
- [21] J. Shi and C. Tomasi. Good features to track. In *IEEE Computer Society Conference on Computer Vision and Pattern Recognition (CVPR'94)*, pages 593–600, Seattle, Washington, June 1994. IEEE Computer Society.
- [22] P. Sturm. Critical motion sequences for monocular self-calibration and uncalibrated Euclidean reconstruction. In *IEEE Computer Society Conference on Computer Vision and Pattern Recognition (CVPR'97)*, pages 1100–1105, Puerto Rico, June 1997. IEEE Computer Society.
- [23] R. Szeliski. Shape from rotation. In *IEEE Computer Society Conference on Computer Vision and Pattern Recognition (CVPR'91)*, pages 625–630, Maui, Hawaii, June 1991. IEEE Computer Society Press.
- [24] R. Szeliski and J. Coughlan. Hierarchical spline-based image registration. In *IEEE Computer Society Conference on Computer Vision and Pattern Recognition (CVPR'94)*, pages 194–201, Seattle, Washington, June 1994. IEEE Computer Society.
- [25] R. Szeliski and S. B. Kang. Recovering 3D shape and motion from image streams using non-linear least squares. *Journal of Visual Communication and Image Representation*, 5(1):10–28, March 1994.
- [26] Z. Zhang. Scaled Euclidean 3D reconstruction based on externally uncalibrated cameras. In *IEEE International Symposium on Computer Vision*, pages 37–42, Coral Gables, Florida, November 1995.





**Quasi-Euclidean Recovery from  
Unknown but Complete Orbital  
Motion**

Sing Bing Kang

**CRL 97/10**

October 1997